CORA Cork Open Research Archive
Cartlann Taighde Oscailte Chorcaí

Title	Improving dynamic endurance time predictions for shoulder fatigue: A comparative evaluation
Authors	O'Sullivan, Patricia;Menolotto, Matteo;O'Flynn, Brendan;Komaris, Dimitrios-Sokratis
Publication date	2025-02-24
Original Citation	O'Sullivan, P., Menolotto, M., O'Flynn, B. and Komaris, D. S. (2025) 'Improving dynamic endurance time predictions for shoulder fatigue: A comparative evaluation', Applied Ergonomics, 125, p.104480 (11pp). https://doi.org/10.1016/j.apergo.2025.104480
Type of publication	Article (peer-reviewed);journal-article
Link to publisher's version	10.1016/j.apergo.2025.104480
Rights	© 2025, The Authors. Published by Elsevier Ltd. This is an open access article under the CC BY license (http://creativecommons.org/licenses/by/4.0/) - https://creativecommons.org/licenses/by/4.0/
Download date	2026-11-01 22:26:50
Item downloaded from	https://hdl.handle.net/10468/17135

UCC
University College Cork, Ireland
Coláiste na hOllscoile Corcaigh

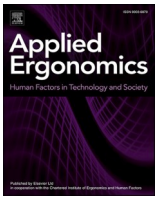
Applied Ergonomics 125 (2025) 104480



Contents lists available at ScienceDirect

Applied Ergonomics

journal homepage: www.elsevier.com/locate/apergo



Improving dynamic endurance time predictions for shoulder fatigue: A comparative evaluation

Patricia O'Sullivan [a,*], Matteo Menolotto [a], Brendan O'Flynn [a], Dimitrios-Sokratis Komaris [b]

[a] Tyndall National Institute, University College Cork, Cork, T12 R5CP, Ireland
[b] Centre of Research and Technology Hellas (CERTH), Marousi, 151 25, Greece

ARTICLE INFO

Keywords:
Upper limb
Physical fatigue
Injury prevention
Occupational health and safety

ABSTRACT

Work-related musculoskeletal disorders (WMSDs) are commonplace in industry and a host of qualitative and quantitative approaches have been used to assuage the problem, including wearable sensors and biomechanical endurance models, both of which were used in the present study. Six endurance models (consumed endurance, new improved consumed endurance and the exponential and power Frey Law and Avin general and shoulder models) with four alternative maximum torque ($Torque_{max}$) quantification methods, including a novel approach to generate $Torque_{max}$, were compared. The proposed approach to quantify $Torque_{max}$, in combination with the new improved consumed endurance model produced the lowest root mean square errors (RMSE), and indicated improved performance compared to the literature. The mean RMSE was reduced from 41.08s to 19.11s for all subjects, from 26.13s to 12.16s for males, and 51.28s to 24.45s for females using the proposed method. R^2 for 25% and 45% standardised intensity dynamic tasks were .459 and .314 respectively, $P < .01$. This research provided an optimised and individualised endurance prediction approach for loaded dynamic movements which can be applied to industry tasks and may lead to reduced upper-limb strains, and potentially WMSDs.

List of Abbreviations

ET	Endurance time
MVC	Maximum voluntary contraction
$Force_{max}$	Maximum force
$Torque_{max}$	Maximum torque
SI	Standardised intensity, $\frac{Force_{load}}{Force_{max}}$
S25	Static task at 25% SI
S45	Static task at 45% SI
D25	Dynamic task at 25% SI
D45	Dynamic task at 45% SI
TT	*True Torque*, $\frac{Torque}{Torque_{max}}$
TT_1	TT calculated using measured shoulder MVC for $Torque_{max}$
TT_2	TT calculated using measured elbow MVC for $Torque_{max}$
TT_3	TT calculated using gender-based MVC values for $Torque_{max}$
TT_{cal}	TT calculated using the calibration task

1. Introduction

Work-related musculoskeletal disorders (WMSDs) are a leading cause of workplace absences and disability, imposing substantial financial burdens on organizations and individuals alike (Crawford et al., 2020), (James et al., 2018). WMSDs, especially those affecting the upper extremities (European Foundation for the Improvement of Living and Working Conditions, 2017), result from repetitive movements (European Foundation for the Improvement of Living and Working Conditions, 2017), (European Agency for Safety and Health at Work, 2022), (Gallagher et al., 2018), (Lind et al., 2023), (Latko et al., 1999), (Silverstein et al., 1987), excessive load (European Agency for Safety and Health at Work, 2022), (Silverstein et al., 1987), (Radwin et al., 2001), sustained contractions (Lind et al., 2023), (Radwin et al., 2001), and awkward postures (European Foundation for the Improvement of Living and Working Conditions, 2017), (Lind et al., 2023), (Keyserling et al., 1992) and are prevalent in manufacturing settings (Crawford et al., 2020), (Singh et al., 2022). Furthermore, Industry 4.0 environments can lead to increased demands, causing the work pace to speed up (Luopajärvi et al., 1979), leading to increased cognitive demands (Madonna et al., 2019), stress (Bispo and Amaral, 2024), and physical fatigue (Bałys et al., 2020), (Lu et al., 2017), thus WMSDs have

* Corresponding author.
E-mail address: patricia.osullivan@tyndall.ie (P. O'Sullivan).

https://doi.org/10.1016/j.apergo.2025.104480
Received 20 August 2024; Received in revised form 7 February 2025; Accepted 12 February 2025
Available online 24 February 2025
0003-6870/© 2025 The Author(s). Published by Elsevier Ltd. This is an open access article under the CC BY license (http://creativecommons.org/licenses/by/4.0/).

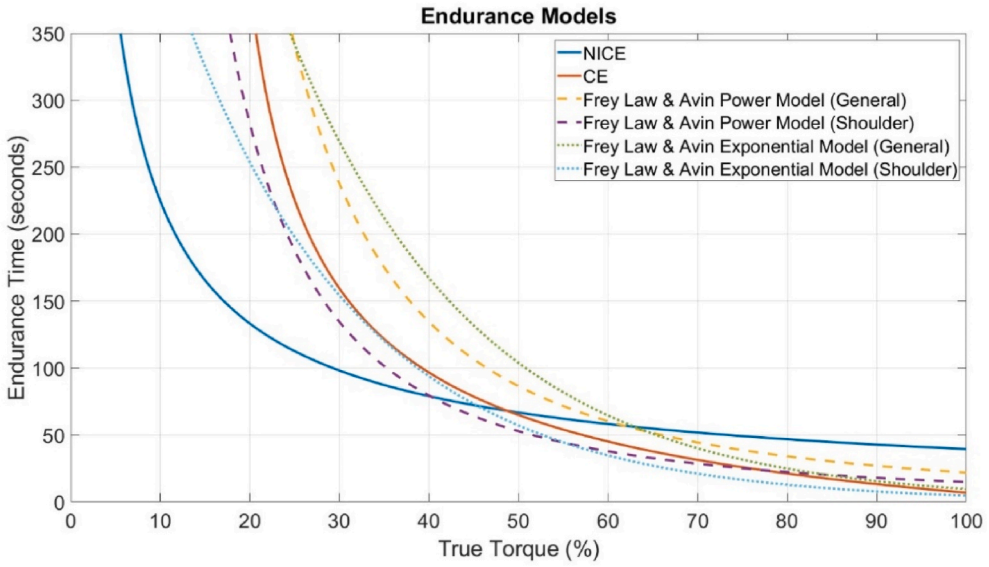


Fig. 1. All six endurance models that are assessed in the study, all are in terms of torque/maximum torque.

detrimental impacts on worker wellbeing. Organizations are impacted by costs due to absences (Crawford et al., 2020), reduced quality (Yung et al., 2020) and efficiency (Williamson et al., 2011) in work output and increased accidents (Williamson et al., 2011). Therefore, WMSD prevention by means of fatigue management serves to benefit all stakeholders.

Fatigue is a complex phenomenon that can be categorised into mental fatigue, drowsiness, physical fatigue and muscle fatigue (Williamson et al., 2011), the latter is characterised by the decreased ability to produce maximum force (Wan et al., 2017), or the required or expected force (Edwards et al., 1981), and was the focus of this study. Fatigue is influenced by a variety of factors, including work-related factors such as heavy loads (Crawford et al., 2020), task complexity and mental stimulation (Williamson et al., 2011), lifestyle factors such as smoking and high body mass index (Crawford et al., 2020), and individual factors such as sex, age, general health (Crawford et al., 2020) and sleep homeostasis (Williamson et al., 2011), (Dawson et al., 2011). These interrelated factors complicate the quantification of fatigue, making effective management challenging. Current research methods to mitigate fatigue-related risks include subjective questionnaires (Borg, 1982), (Åkerstedt and Gillberg, 1990), (Hart and Staveland, 1988), maximum allowable weight tables (Snook and Ciriello, 1991), ergonomic risk assessments (Steven Moore and Garg, 1995), (McAtamney and Hignett, 2004), (McAtamney and Corlett, 2004), (Waters et al., 1993), endurance models (Rohmert, 1960), (Rohmert, 1973), (Frey Law and Avin, 2010), (Mathiassen and Åhsberg, 1999), and muscle models, (Ma et al., 2009), (Liu et al., 2002), (Jang et al., 2017), (Jebelli et al., 2020), these models quantify fatigue by simulating muscle states due to external forces, the accumulation of metabolites, or force-pH relationships (Yu et al., 2019). However, there is considerable debate regarding the generalizability and reliability of the methods, highlighting the need for alternative approaches that offer more personalized and accurate fatigue assessments.

Endurance models, represented by power or exponential curves, depict the reduced capacity to sustain work at higher loads relative to an individual's maximum producible force and estimate endurance time (ET). These models are often tailored to specific joints, ranges of motion, and task types (Frey Law and Avin, 2010), (El ahrache et al., 2006), (Garg et al., 2002), (Li et al., 2021), (Yi et al., 2018), and assume constant force (Duan et al., 2020), therefore they are applicable to isometric conditions and in some cases have been valid for slow isokinetic tasks (Hagberg, 1981). While muscle models can be applicable to dynamic tasks, they typically estimate current fatigue level or maximum exertable force rather than predicted ET and often have complex equations with multiple parameters that make real-time integration difficult (Yu et al., 2019).

Endurance models have been adapted to design human-machine interfaces that minimize fatigue. The consumed endurance (*CE*) model (Equation (1), orange line in Fig. 1), derived from Rohmert's model (Rohmert, 1960) for static tasks, replaces $\frac{Force}{Force_{max}}$ with $\frac{Torque}{Torque_{max}}$ to capture changes in the moment arm, offering fatigue assessment for dynamic conditions. The *CE* model was applied in unloaded conditions (Hincapié-Ramos et al., 2014) and in loaded conditions with high errors (O'Sullivan et al., 2023), and there are disagreements regarding the fixed asymptote (minus 15 in the denominator) not reflected in recent empirical findings (Mathiassen and Åhsberg, 1999), (El ahrache et al., 2006), (Li et al., 2023). The new improved consumed endurance (*NICE*) model (Equation (2), blue solid line in Fig. 1), addressed these limitations by removing the asymptote and fitting a power curve to experimental data (Li et al., 2023).

$$ET_CE = \frac{1236.5}{\left(\frac{Torque}{Torque_{max}} \times 100 - 15\right)^{0.618}} - 72.5 \quad (1)$$

$$ET_NICE = \frac{1277.9066}{\left(\frac{Torque}{Torque_{max}} \times 100\right)^{0.7546}} \quad (2)$$

Frey Law and Avin (Frey Law and Avin, 2010) offered a comprehensive meta-analysis of maximum ET models by fitting power and exponential curves to empirical endurance data from multiple studies. The Frey Law & Avin power ($ET = b0*(MVC)^{b1}$) and exponential ($ET = b0*exp^{(MVC*b1)}$) models contain coefficients ($b0$ and $b1$) that describe endurance for different joints as well as generalised curves for the whole body in terms of maximum voluntary contraction (MVC) force percentage, also referred to as standardised intensity (SI). For example, the general power model was expressed as $ET = 21.92*MVC^{-1.98}$ and, similar to the *CE* model (Equation (1)) which replaced force inputs in Rohmert's model (Rohmert, 1960) with torque inputs, the force inputs were replaced with torque inputs in these general and shoulder power models (Equations (3) and (4)) and general and shoulder exponential models (Equations (5) and (6)) in this work.

Table 1
Anthropometric and demographic data of participants.

Subject Details			
Parameters	All Subjects	Males	Females
Age (years)	27.7 ± 4.3	28.5 ± 3.6	26.9 ± 4.8
Height (m)	1.72 ± .09	1.78 ± .07	1.65 ± .04
Body Mass (kg)	70.48 ± 13.13	78.41 ± 11.11	61.99 ± 9.25
Body Mass Index (kg/m^2)	23.70 ± 3.13	24.55 ± 2.77	22.81 ± 3.25
Fat %	26.95 ± 7.82	22.64 ± 6.54	31.56 ± 6.28
Muscle %	33.27 ± 5.71	37.66 ± 3.82	28.56 ± 3.01
Upper Arm Length (m)	.34 ± .04	.36 ± .04	.33 ± .03
Forearm Length (m)	.26 ± .03	.28 ± .04	.25 ± .02
Hand Length (m)	.18 ± .01	.18 ± .01	.18 ± .01
Shoulder MVC (N)	62.88 ± 23.81	82.78 ± 15.15	41.55 ± 7.04
Elbow MVC (N)	112.23 ± 53.17	152.69 ± 43.37	68.88 ± 14.43

$$ET_FA_Power_{General} = \frac{21.92}{\left(\frac{Torque}{Torque_{max}}\right)^{1.98}} \quad (3)$$

$$ET_FA_Power_{Shoulder} = \frac{14.86}{\left(\frac{Torque}{Torque_{max}}\right)^{1.83}} \quad (4)$$

$$ET_FA_Exp_{General} = \frac{1122.32}{e^{\left(\frac{Torque}{Torque_{max}}\right)\times 4.76}} \quad (5)$$

$$ET_FA_Exp_{Shoulder} = \frac{685.46}{e^{\left(\frac{Torque}{Torque_{max}}\right)\times 4.97}} \quad (6)$$

This study built on previous research (O'Sullivan et al., 2023) and compared torque-based endurance models (Equations (1)–(6), curves in Fig. 1) and four methods of obtaining $Torque_{max}$ to assess their predictive accuracy for fatiguing static and dynamic tasks. The goal was to determine the most effective models and inputs for predicting ET and to address the limitations of current methods by developing a more individualised approach. By focusing on fundamental tasks, this research aimed to lay the groundwork for applying these models to more complex industrial tasks.

2. Material and methods

Subject parameters, ET and optical motion capture (MoCap) data for shoulder tasks were extracted from an open-access dataset (O'Sullivan, 2024) which also includes additional tasks and sensor data.

2.1. Participants

Twenty-nine participants (14 females) were recruited by word of mouth and provided written, informed consent to take part in the study. The protocol herein received approval from the university's ethics committee (CREC Review Reference number: ECM4(p)July 6, 2021). Participants were asked to attend the session fully rested and completed a 5-min upper body warm-up prior to data capture. Demographics and anthropometrics were gathered (Table 1) using the clinically validated OMRON BF511 Body Composition Monitor (Omron Corporation, Kyoto, Japan) (Bosy-Westphal et al., 2008) and anthropometric measuring tape following measurement guidelines (Garrett, 1971), (Neumann et al., 2018).

2.2. Maximum forces and sensor set-up

MVCs of the shoulder and elbow joints in flexion (Table 1) were measured using a loadcell (range = 30 kg; accuracy = .02%; non-linearity = .02% F.S.). For shoulder MVC, participants' arms were outstretched with the shoulder joint flexed at 90°, hand in supination, and upper limb joints in alignment. For elbow MVC, the elbow was flexed at 90°, hand in supination, and elbow and wrist joints in alignment with the loadcell. MVCs and tasks were completed with the dominant arm which was defined as the arm used to perform daily tasks. Participants pushed upwards against the loadcell using maximum effort for 3 s while maintaining a straight posture three times (Ma et al., 2013), firstly for a practice test, and forces were recorded on the second and third attempts with a 2-min break in between (Freivalds, 2011, p. 78), the mean of which was used to determine MVC. The closest weights to 25% and 45% SI, determined the dumbbell weight lifted during tasks in the study, available weights (in kg) were .5, 1, 2, 3, 4, 5, 6, 7.5, 10, corresponding closely to the desired SI, and actual SIs are shown in Table 2. The closest dumbbell load was typically below the desired SI for females (for example, 25% SI corresponded to 1.17 kg for one subject and this was rounded down to the available 1 kg load, resulting in an actual SI of 21.33%) and the opposite was true for males, explaining the differences in actual and desired SI between sexes.

Table 2
Ideal and real standardised intensities (%) of the loads lifted in the study.

Standardised Intensities (%)			
Ideal SI	All Subjects	Males	Females
25	24.5 ± 3.8	27.1 ± 3.4	21.9 ± 2.0
45	44.5 ± 4.5	45.8 ± 4.6	43.7 ± 4.0

Ten Prime 13 and 2 Prime 13X OptiTrack cameras (NaturalPoint, Inc., Corvallis, OR, USA), sampling at 180Hz, obtained motion data required for calculating *Torque*. The highest mean calibration ray error was .6 mm and mean calibration wand error was .1 mm. A 27-marker set by Optitrack ('Conventional Upper Skeleton Marker Set) was utilised, enabling tracking of the upper body. Markers were attached to the participant using double sided sticky tape and Velcro.

2.3. Tasks

Subjects completed four tasks, Fig. 2:

- Static at 25% (S25); the shoulder joint was flexed 90° to the trunk with the arm outstretched, dumbbell was hand-held in a supinated position, posture was upright.
- Dynamic at 25% (D25); the shoulder joint was continuously flexed between 0 and 90°, where the arm was down by the individual's side at 0°, and in the static task position at 90°.
- Tasks were repeated at 45% load intensity, called S45 and D45.

Other tasks are included in the dataset (O'Sullivan, 2024), and were completed in two different orders, refer to the dataset for more information. Furthermore, these tasks involve minimal complexity, providing a basic platform to test and compare the models, and an elevation action such as this is relevant to manual handling and assembly tasks. SIs of 25% and 45% were chosen as there is a rapid decrease in endurance curves around 15–20% SI due to the ischemic effect as a result of intramuscular pressure (Hagberg, 1981), and there is much disagreement about ETs in this range, as previously mentioned. 25% was chosen as the first SI to attain an idea of ETs after this rapid decrease, and 45% was chosen as ETs reduce significantly beyond 50% SI.

For the 25% SI tasks, Borg RPE (Borg, 1982) scores (ranging from 6 to 20) were attained before the task, 5 s into the task, at 15 s, and every 15 s thereafter. For 45% SI tasks, Borg RPE score was acquired before the task, at 5 s, 10 s and every 10 s thereafter (Garg et al., 2002). Experimental ET was recorded as the time taken to reach a fatigued state, indicated by Borg RPE score $\geq$ 17 (Martins et al., 2021) or when the

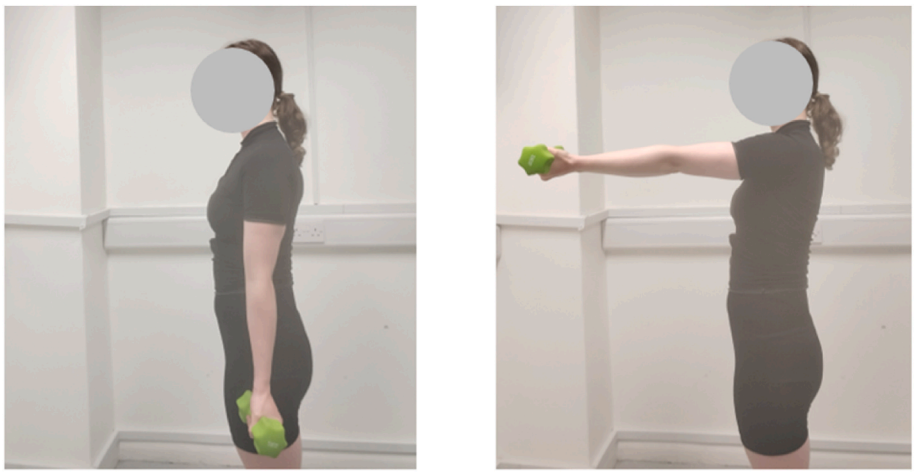


Fig. 2. Arm position at (left) 0° and (right) 90° during the tasks. During the static task, the 90-degree position is maintained while the arm is flexed between 0 and 90° during the dynamic task at 50 beats per minute.

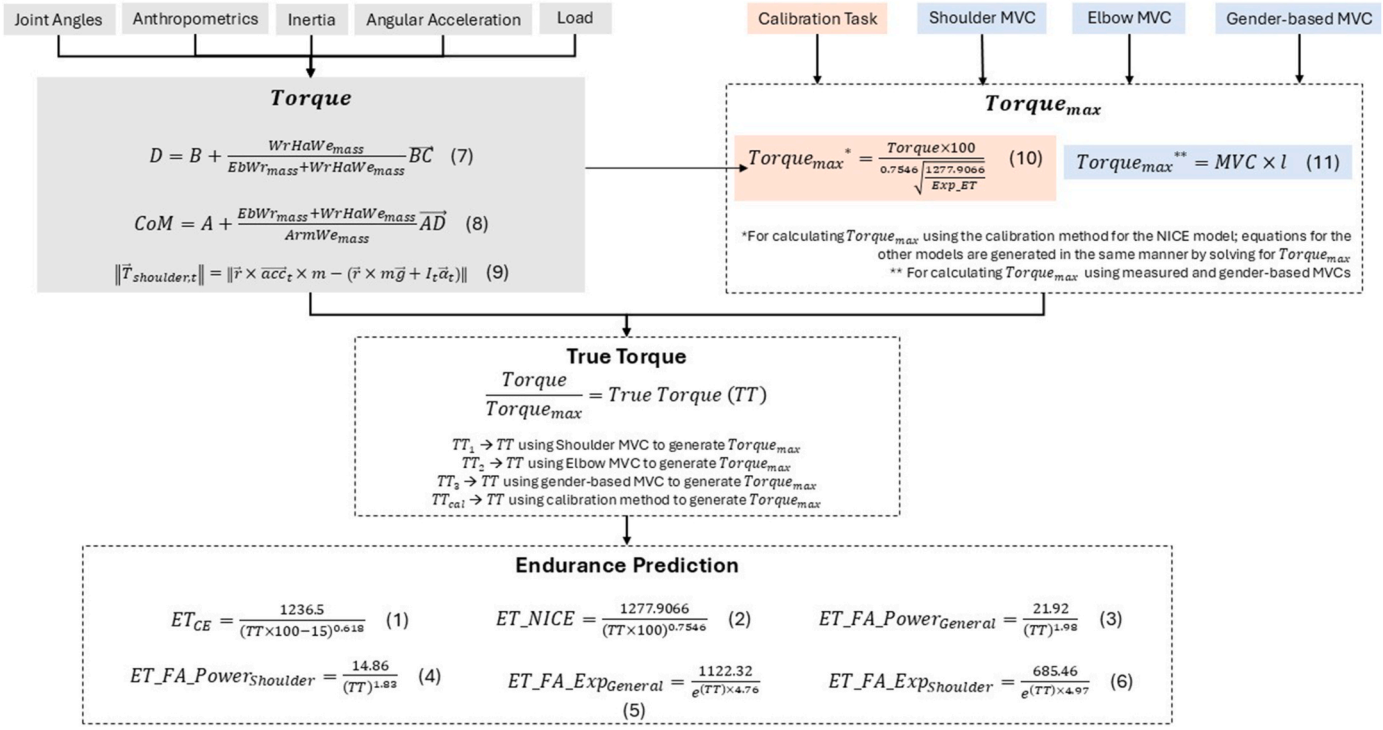


Fig. 3. Procedure for calculating predicted endurance times for each of the six endurance models with four methods of obtaining maximum torque, resulting in 6 × 4 = 24 different RMSE values.

correct form could no longer be maintained (Li et al., 2023). Measuring maximum holding time is a common method used to generate endurance curves (Frey Law and Avin, 2010), (El ahrache et al., 2006), (Li et al., 2023). Since endurance models were valid for 2 s cycles in previous research (Hagberg, 1981), a slightly faster rate (50 beats per minute) which still encouraged controlled movement was maintained using a metronome, as quicker movements more closely resemble the rate of real-world occupational tasks. 7.5- and 10-min breaks were provided for tasks at 25% and 45% SI (Ma et al., 2013) and tasks could only begin when Borg RPE was 6–7, indicating a rested state.

2.4. Analysis

Predicted ET was found using six models (Equations (1)–(6)) and four methods of obtaining $Torque_{max}$, Fig. 3. *True Torque* (TT) is the required input to all models and is expressed as $\frac{Torque}{Torque_{max}}$, where *Torque* is the sum of the torques acting on the frontal axis of the shoulder (Equations (7)–(9), (Hincapié-Ramos et al., 2014)) and was calculated using joint angles extracted from MoCap data, anthropometric data (Table 1 and (Winter 2009)), inertia, angular acceleration and dumbbell load, see grey in Fig. 3. $Torque_{max}$ is the maximum torque produced by the individual (Equations (10)-11)), see orange and blue in Fig. 3.

Gaps in the position tracking of markers smaller than 90 samples (~.5 s) were filled using cubic interpolation via Motive software (NaturalPoint, Inc., Corvallis, OR, USA); larger gaps were filled with pattern interpolation using surrounding markers as reference. A 4th degree Butterworth filter with a 6Hz cut-off was used for filtering, takes were

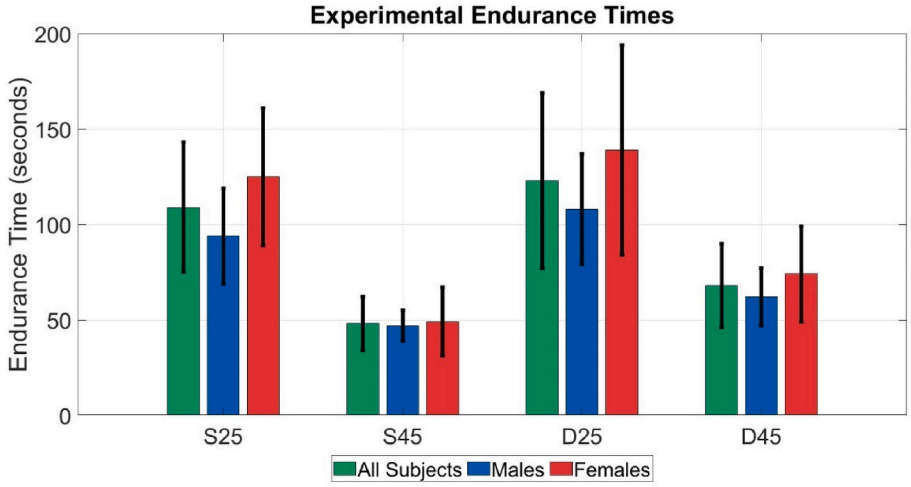


Fig. 4. Mean and standard deviation (black lines) of the experimental endurance times for all tasks for all subjects, males and females.

exported and run through a MATLAB script to extract joint angles. A simplified approach entailed creating vectors for arm segments using shoulder, elbow, wrist and finger markers and the angle between them were found in frontal plane. Angles and anthropometric data were used to calculate the centre of mass (CoM) of the system using Equations (7) and (8), where A, B and C are the CoMs of the upper arm, forearm and hand respectively, D is the CoM of the forearm (EbWr) and hand and weight (WrHaWe), the dumbbell was assumed to act at the CoM of the hand. r is the distance from the shoulder to the CoM, the inertia of the arm segments was found similar to (Winter 2009) and the dumbbell was approximated as a sphere. $\overrightarrow{acc}$ is the acceleration of the CoM and angular acceleration α was found using $\frac{\overrightarrow{acc}}{\|\overrightarrow{r}\|}$.

$$D = B + \frac{WrHaWe_{mass}}{EbWr_{mass} + WrHaWe_{mass}}\overrightarrow{BC} \tag{7}$$

$$CoM = A + \frac{EbWr_{mass} + WrHaWe_{mass}}{ArmWe_{mass}}\overrightarrow{AD} \tag{8}$$

$$\left\|\overrightarrow{T}_{shoulder,t}\right\| = \left\|\overrightarrow{r} \times \overrightarrow{acc}_t \times m - \left(\overrightarrow{r} \times m\overrightarrow{g} + I_t\overrightarrow{\alpha}_t\right)\right\| \tag{9}$$

While *Torque* can be calculated from MoCap data, this method of calculating *Torque* takes the hand-held load into account and can be used with wearables, such as IMUs, which future work aims to incorporate. *Torque* remains approximately constant throughout the static tasks (as rotational equilibrium is maintained) and it fluctuates throughout each cycle in the dynamic tasks as CoM changes. Since $Torque_{max}$ is a constant, predicted ET remains fairly constant for static tasks and fluctuates throughout dynamic tasks.

Since the calculation of *Torque* remains consistent, *TT* varies depending on the method to determine $Torque_{max}$. For TT_1, TT_2 and TT_3, $Torque_{max}$ was approximated by multiplying MVC by arm length, the latter of which was the distance from the relevant joint to mid-palm, Equation (11), Fig. 3. However, different methods of quantifying MVC exist among endurance studies. MVC was measured from the shoulder joint in the *NICE* study (Li et al., 2023), while the *CE* study (Hincapié-Ramos et al., 2014) used 101.6N for males and 87.2N for females from elbow MVC tables (Tan et al., 1994). Measured MVC from the shoulder (TT_1) and elbow (TT_2) and sex-based tables (TT_3) were used to generate three sets of *TTs*. Although tasks in this study focussed on shoulder elevation, elbow MVC was included as this joint was used in the *CE* study (Hincapié-Ramos et al., 2014) which included similar tasks.

A new method of obtaining *TT* using a calibration task, which we called TT_{cal}, was compared to the aforementioned *TTs* (TT_1, TT_2, TT_3). Instead of measuring MVC, generating TT_{cal} used a calibration task to determine the $Torque_{max}$ that resulted in the correct ET prediction for the calibration task conditions; this $Torque_{max}$ was then used to predict the ET for all other tasks, see orange section in Fig. 3. In other words, the *Torque* and experimental ET of the calibration task were inputted into the models that were rearranged to solve for $Torque_{max}$, Fig. 3 shows an example with the *NICE* model (Equation (10)). The process was completed using all models resulting in six TT_{cal} per calibration task.

All tasks were assessed on their ability to perform as a calibration task; mean and absolute mean ET errors (%) were used to compare the predictive ability of the tasks to determine which ones perform most effectively as calibration tasks. The *TTs* (TT_1, TT_2, TT_3 and TT_{cal}) were then inputted into each of the six models (Equations (1)–(6)) and the ability of different models and *TTs* to predict the experimental ETs of the participants were compared. In this way, the impact of $Torque_{max}$ on ET prediction of the models can be ascertained, and the optimal *TT* and model can be selected.

MATLAB Curve Fitter was used to assess the fit of experimental data to the curves. All subjects were analysed, then males and females were analysed separately, firstly for all tasks, then in the following groups: static and dynamic tasks, and tasks at 25% and 45% SI. Root mean squared errors (RMSEs) of the *TTs* with all six models were examined to understand the impact of $Torque_{max}$ on ET predictions and to identify which models, *TTs* and model-*TT* combinations (e.g. *CE*-TT_1 meaning TT_1 was inputted to the *CE* model) resulted in the lowest error for each sex, movement, and load category. This information may be used to inform which models and *TTs* are best suited to a specific cohort of individuals under specific movement or load conditions. Experimental data from the *NICE* study (Li et al., 2023) were shared with the authors, to enable RMSE comparisons to be made with the present work.

3. Results

3.1. Personal factors

Mean experimental ETs across all tasks were slightly higher for females (Fig. 4). At best, moderate Pearson correlation coefficients were achieved when analysing the relationship between personal factors and experimental ETs, showing moderate negative relationships between muscle % and S25, D25 or D45 (>-.394, $P < .05$), and moderate positive relationships between fat % and D25 or D45 (>.427, $P < .05$).

3.2. Calibration task selection

To determine which tasks performed best as calibration tasks, we

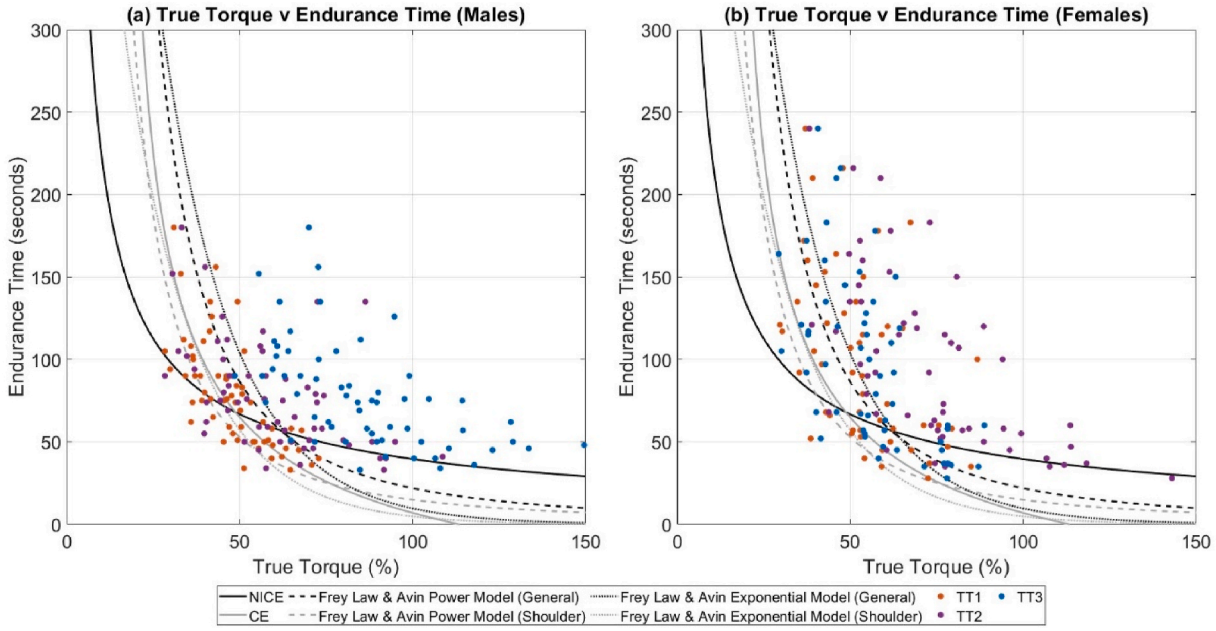


Fig. 5. Different methods of determining maximum torque result in dramatically different true torques, the variable used to calculate endurance prediction time, for both (a) males and (b) females.

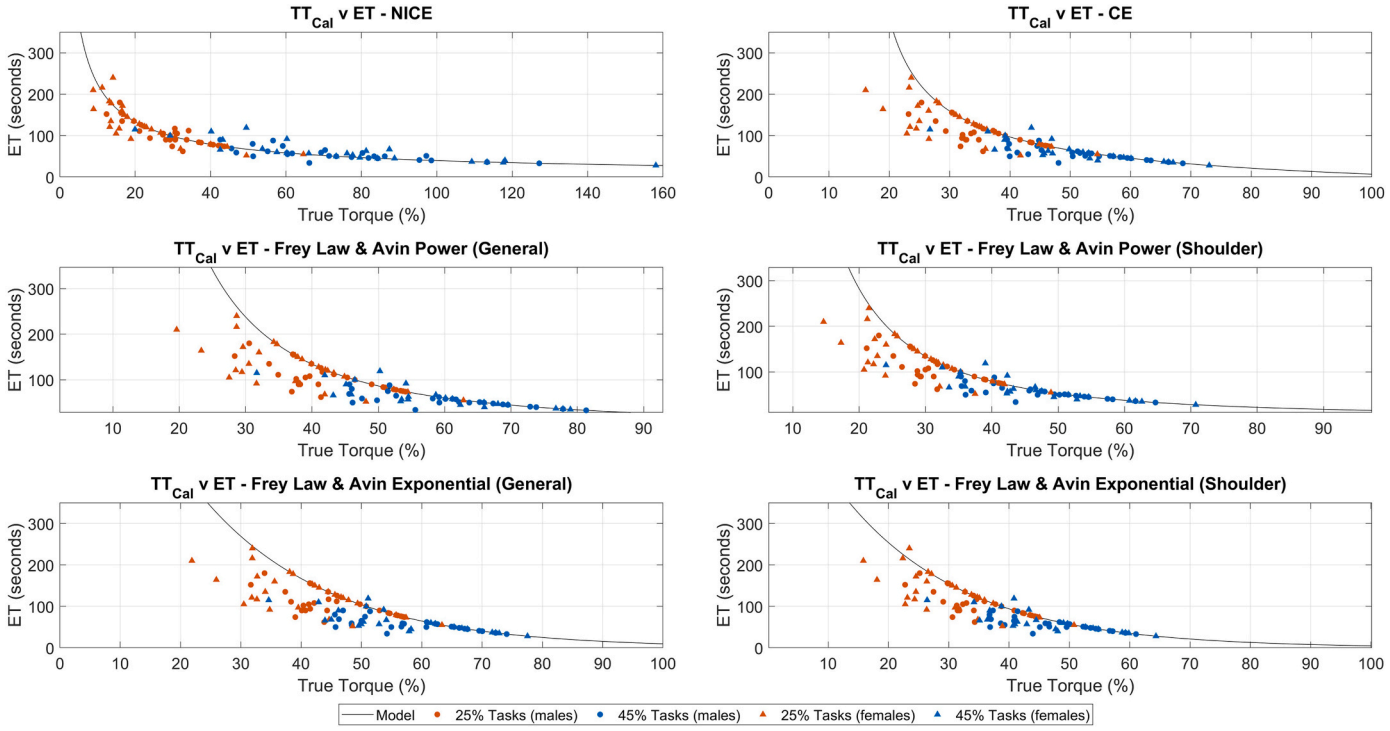


Fig. 6. Calibration true torques plotted against experimental endurance times for all models. Static tasks appear on the model curve while dynamic tasks deviate slightly as their true torque was calculated using the torque max of the static task at that load.

analysed which one (S25, S45, D25, D45) returned the TT_{cal} that yielded the lowest error in the predicted ETs for all other tasks. This was tested on all six models to compare how models perform with a calibration task. Overall, D45 performed best across all models, producing absolute mean ET errors between 20.6% and 22.2%. Following this, tasks were grouped based on load, meaning only 25% SI tasks were used to predict ET of 25% SI tasks and the same for 45% SI tasks, this approach reduced errors compared to using D45 as the calibration task. For 25% SI tasks, *NICE* with D25 claimed the lowest mean absolute error (9.5%), while *NICE* with S25 was at 11.7%; S25 performed better than D25 across all other models but with higher mean absolute errors than the *NICE* model. For the 45% SI group: D45 performed better than S45 in all models except for *NICE*, where *NICE* achieved the lowest error across all models in this load group with an absolute mean error of 9.8% for S45 and 11.8% for D45. Based on this information and the ease of replication of static compared to dynamic tasks, S25 and S45 were selected as calibration tasks for their respective load groups. This means that the $Torque_{max}$ generated for each model using tasks S25 and S45 were used

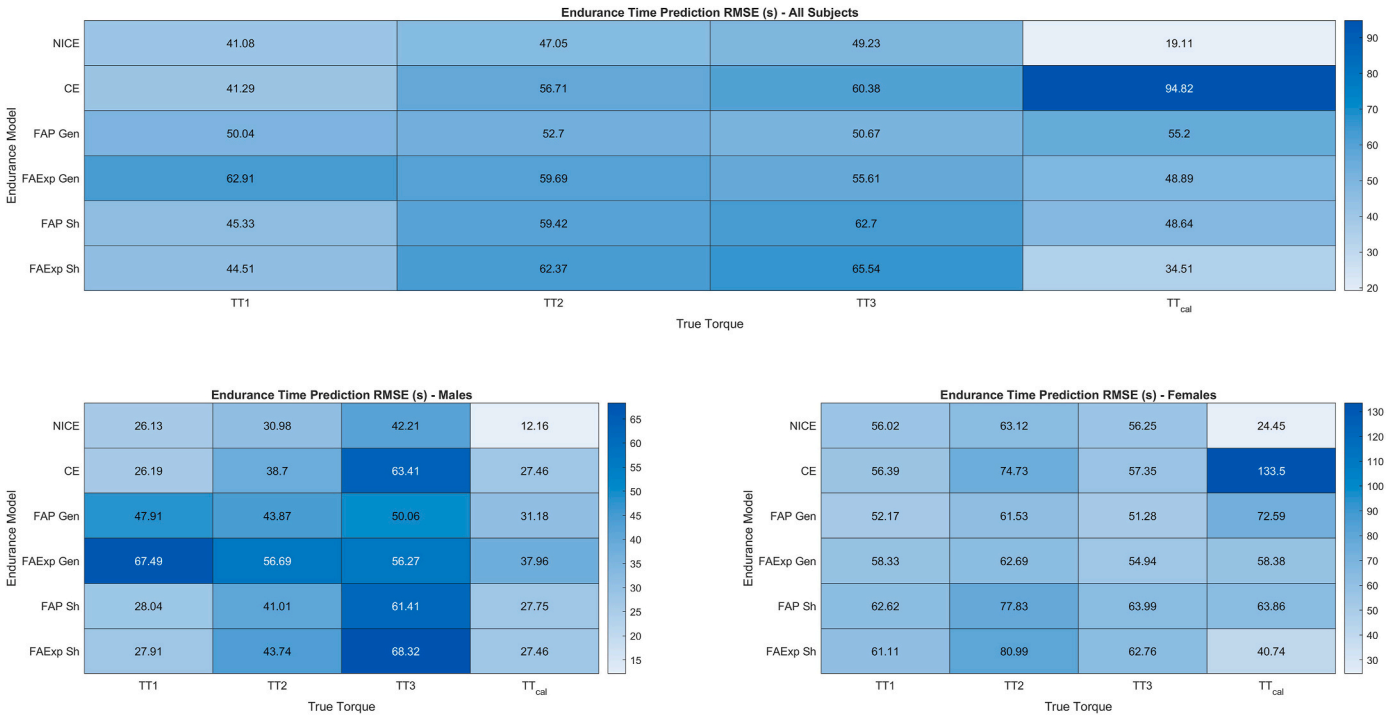


Fig. 7. RMSEs for each model and true torque combination for all tasks, for (a) all subjects, (b) males, (c) females. FAP Gen = Frey Law and Avin general power model, FAExp Gen = Frey Law and Avin general exponential model, FAP Sh = Frey Law and Avin shoulder power model, FAExp Sh = Frey Law and Avin shoulder exponential model.

to generate TT_{cal}, as per Fig. 3, to predict ETs for all tasks at that load.

3.3. Influence of TT, sex and task type

TTs were plotted against experimental ET (Fig. 5 for TT_1 to TT_3 and Fig. 6 for TT_{cal}), firstly, to show the difference between experimental ETs (data points) and predicted ETs according to the endurance models (solid and dashed curves, (Frey Law and Avin, 2010), (Hincapié-Ramos et al., 2014), (Li et al., 2023)); secondly, to show how *TT* influenced predictions; and finally, to show load, movement and sex differences. Mean predicted ET was plotted in Figs. 5 and 6 and since the mean *Torque* resulted in the mean predicted ET for both tasks, mean *Torque* was divided by $Torque_{max}$ to generate *TT* for these figures. For Fig. 5, *TTs* were labelled depending on MVC, where *TTs* from measured shoulder and elbow MVCs were TT_1 (red) and TT_2 (purple), respectively, and TT_3 (blue) were calculated using literature-reported sex-based MVCs (Tan et al., 1994). We see that *TT* and sex, males in (a) and females in (b), greatly impacted predicted ET; for example, TT_3 resulted in a worse fit to the models than TT_1 and TT_2 for males; the wide range of female experimental ETs made it difficult to determine which model and *TT*, if any, were best suited to predicting ET; saying this, TT_3 fitted the models for females better than males. Even though the real SIs were within 5% of the

target SIs (Table 2), the *TT* range was much greater than this due to the influence of parameters that were used to calculate *Torque*, such as arm mass and arm length.

In Fig. 6, each model is shown individually because a different $Torque_{max}$ depending on the model in question; a sex breakdown is also provided (circles for males, triangles for females). Static tasks appear on the model curve since these tasks were used to generate the $Torque_{max}$ that delivered 0% error, while dynamic tasks appear close to the curves, often following a consistent trajectory, with females deviating further from the curve in general than males with D25. Models typically overestimated the ET of dynamic tasks with this method because experimental ET of dynamic tasks (represented by data points) mostly fall under the predicted ET values (represented by curves), except for the *NICE* model where there seems to be a more even distribution of data points. This is the opposite for TT_1, TT_2 *and* TT_3 as they frequently underestimated ETs (Fig. 5), particularly for TT_3 with males and for TT_2 with females.

The fit of experimental data (using $TT_1, TT_2, TT_3, TT_{cal}$) to each of the models resulted in 24 RMSEs each for the following categories: all tasks, static tasks, dynamic tasks, tasks at 25% and 45% SI, for all subjects, males and females. Fig. 7, S1 and S2 (the latter two are in Supplementary Materials) show the RMSEs across all categories, highlighting the models, *TTs*, and model–*TT* combinations that resulted in the lowest errors. Across all tasks and subjects (Fig. 7), *NICE*-TT_{cal} performed the best and lowest RMSEs were generated with this model-*TT* combination (RMSE is 19.11s for all subjects, 12.16 s for males and 24.45 s for females). The TT_{cal} column in Fig. 7 includes the combined RMSE of static and dynamic task, note the 0 s RMSE for static tasks using TT_{cal}, as shown in Fig. S1 (a) and (c) which gives a breakdown of static and dynamic tasks by sex. For dynamic tasks (Fig. S1 (b) and (d)), *NICE*-TT_{cal} remains the best performing model-*TT* combination, where the best RMSE for females was reduced from 56.20 s (best model-*TT* without TT_{cal}) to 34.58 s (best model-*TT* with TT_{cal}) and for males from 25.21 s (best model-*TT* without TT_{cal}) to 17.19 s (best model-*TT* with TT_{cal}).

Fig. S2 shows a breakdown of SI and sex, where *NICE*-TT_{cal} resulted in the lowest RMSEs for males (14.31 s) and females (31.07 s) for both tasks at 25% SI (S25 and D25), and the remaining model-*TT* combinations span the following ranges, 32.41 s ($FA_Exp_{Shoulder}$-TT_{cal}) to 85.81 s ($FA_Exp_{General}$-*TT* 1) for males and 52.44 s ($FA_Exp_{Shoulder}$-TT_{cal}) to 187.50 s (*CE*-TT_{cal}). Similar to 25% SI tasks, *NICE*-TT_{cal} resulted in the lowest RMSEs for males (9.53 s) and females (15.18 s) for 45% SI tasks, Fig. S2. Remaining model-*TT* combinations for 45% SI tasks ranged from 12.26 s (*NICE*-*TT*2) to 49.05 s ($FA_Exp_{Shoulder}$-TT_3) for males and 21.50 s (*CE*-TT_{cal}) to 52.37 s ($FA_Exp_{Shoulder}$-*TT* 2) for females. The introduction of TT_{cal} led to significant reductions of RMSEs across all load levels and subjects. There were consistently higher RMSEs for females at both load levels, however, TT_{cal} narrowed the gap between male and female

errors, especially at 25% SI for females, 67.31 s (best model-*TT* without TT_{cal}) to 31.07 s (best model-*TT* with TT_{cal}). R^2 for *NICE*-TT_{cal} were .459 for D25 and .314 for D45, denoting a weak explanation of the variability in the data.

4. Discussion

4.1. Summary of findings

This study built on previous research (O'Sullivan et al., 2023) and used six torque-based endurance models to predict ET during lifting and highlighted the impact of $Torque_{max}$ measurement. Unlike traditional models that rely on force inputs and focus on one joint or task (Frey Law and Avin, 2010), (El ahrache et al., 2006), (Garg et al., 2002), (Li et al., 2021), (Yi et al., 2018), the described approach accounted for changes in *Torque* and considered three joints in the upper extremities, widening the applicability to tasks with different arm configurations. The study's findings offer practical recommendations for improving ET predictions. By conducting static calibration tasks at multiple load levels researchers can determine the optimal $Torque_{max}$ for lifting tasks in a standardised and easily reproducible manner. Future work will focus on assessing the generalizability of this method to other manual tasks. This approach provides a repeatable method for reducing ET prediction errors and presents potential for improving fatigue management in real-world settings. Furthermore, the predictive output supports the move towards proactive fatigue prevention for dynamic tasks which is lacking in the literature (Kheiri et al., 2023), (Lim and D'Souza, 2020), and previously mentioned methods in current research, such as (Snook and Ciriello, 1991), (McAtamney and Corlett, 2004), (Rohmert, 1960), (Frey Law and Avin, 2010), (Ma et al., 2009), (Jang et al., 2017), do not directly provide.

4.2. Influence of $Torque_{max}$

Results highlighted variations in ET predictions based on the method used to quantify $Torque_{max}$. The *NICE* model, when combined with the calibration approach, demonstrated the lowest prediction errors. The $Torque_{max}$ used to generate TT_1, TT_2, TT_3 with Equation (11), Fig. 3, may have faced error propagation while $Torque_{max}$ achieved by the calibration method did not. Calibration tasks resulted in reduced errors for both static and dynamic tasks, as mean errors (mean absolute errors) were 7.63% (11.65%) for both 25% SI tasks and −4.69% (9.8%) for both 45% SI tasks, where positive values indicate overprediction and negative to underprediction of ET. ET errors were reduced compared to previous work (O'Sullivan et al., 2023) which used the *CE* model to predict ET of fatiguing static and dynamic shoulder elevation using only measured shoulder forces for $Torque_{max}$; mean absolute ET errors (and standard deviations) were 28.62% ± 23.27% for static and 115.45% ± 70.42% for dynamic tasks.

4.3. Static versus dynamic tasks

Fig. 6 revealed that dynamic tasks exhibited a different endurance trajectory compared to static tasks, with lower mean *TT* for dynamic tasks at the same SI, due to *Torque* fluctuating during movement. When the arm is outstretched at 90° from the trunk, *Torque* is at its peak, but *Torque* decreases as the arm moves closer to 0°, primarily because r decreases. Meanwhile, the high *Torque* position was maintained during static tasks, resulting in a shift of the dynamic data points to the left (to this lower *TT*) compared to the static data points completed at the same SI, leading to models generally overpredicting dynamic tasks with TT_{cal} (Fig. 6) which can lead to health and safety concerns in real-world applications (i.e. endurance limit has been reached before the model predicts). However, *NICE*-TT_{cal}, with its lower RMSE, showed a more even distribution of dynamic data points, suggesting a better fit and reduced errors compared to other models, Fig. 6(a). We found that endurance models can predict ET for quicker, more realistically paced tasks for workers compared to force-based models that were valid for static tasks and slow movements with sustained contractions (Hagberg, 1981).

4.4. Model fit and accuracy

Frey Law and Avin models (Frey Law and Avin, 2010) showed R^2 values between .784 and .897 (using force inputs), while the *NICE* model (Li et al., 2023) had an R^2 of .572. In the present study, the best-performing model, *NICE*-TT_{cal} showed lower R^2 values (.459 for D25 and .314 for D45, $P < .01$), although these were for dynamic movements as opposed to static movements in the aforementioned studies. Interestingly, D25 had a better R^2 than D45, although D45 performed better in terms of RMSE. Despite lower R^2, the RMSE of the *NICE*-TT_{cal} model (19.11 s) was significantly lower than the *NICE* model's RMSE (65.23 s) (Li et al., 2023), indicating improved predictive accuracy.

4.5. Personal factors

Mean experimental ETs across all tasks were slightly higher for females (Fig. 4), which is in alignment with studies that found females generally exhibit lower fatiguability than males during isometric tasks at the same SI (Hunter, 2016), (Hunter, 2014) - similar trends were found during some dynamic tasks (Hunter, 2016). Higher sex-based fatiguability differences were observed for lower velocity and SIs, particularly with elbow flexors (Hunter, 2016), (Hunter, 2014), and similar effects may apply to shoulder tasks in the present study. Importantly, muscle group and contraction type affect sex differences, where recovery is slower for females in lengthening activations of some muscle groups (Hunter, 2014), which can be explored in future research. Additionally, lower actual SIs for females compared to males (Table 2) may have impacted differences. The inclusion of torque denoted increased individualisation compared to force-based models due to the inclusion of arm segment lengths and masses in Equations (7)–(9). Contrary to expectations, fat percentage showed a positive relationship with experimental ET, while muscle percentage had a negative relationship. These findings highlight the need for further research to explore the impact of personal factors on endurance.

4.6. Limitations

The number of subjects was in alignment with the literature, but this can vary significantly, ranging from 9 (Hagberg, 1981) and 12 (Garg et al., 2002), (Li et al., 2023) to 40 (Mathiassen and Åhsberg, 1999) and 60 (Liu et al., 2019) participants. A larger dataset could achieve a more representative view of the population, and the narrow age range of subjects (Table 1) does not represent the working population. Measured arm segment lengths could have been considered from the shoulder joint centre (Nussbaum and Zhang, 2000) instead of the acromion. Additional dumbbells, such as a 1.5 kg dumbbell, may have resulted in actual and desired SIs matching more closely (Table 2) and may impact sex-based differences. Despite participants feeling rested before tasks, there may be a cumulative effect of fatigue that potentially resulted in underperformance in final tasks. Other methods of $Torque_{max}$ measurement exist, for example, (Chaffin et al., 1999) determines MVC from loadcell, mass and anthropometrics, and (O'Sullivan et al., 2022) uses height and upper forearm volume. These methods and other maximum ET models, listed in El ahrache et al. (2006), were not considered. A straight-arm configuration was maintained in all tasks without consideration of abduction and bent-arm conditions as was done in the *CE* and *NICE* studies (Hincapié-Ramos et al., 2014), (Li et al., 2023).

4.7. Practical recommendations

New ET models were not developed, instead, alternative inputs and

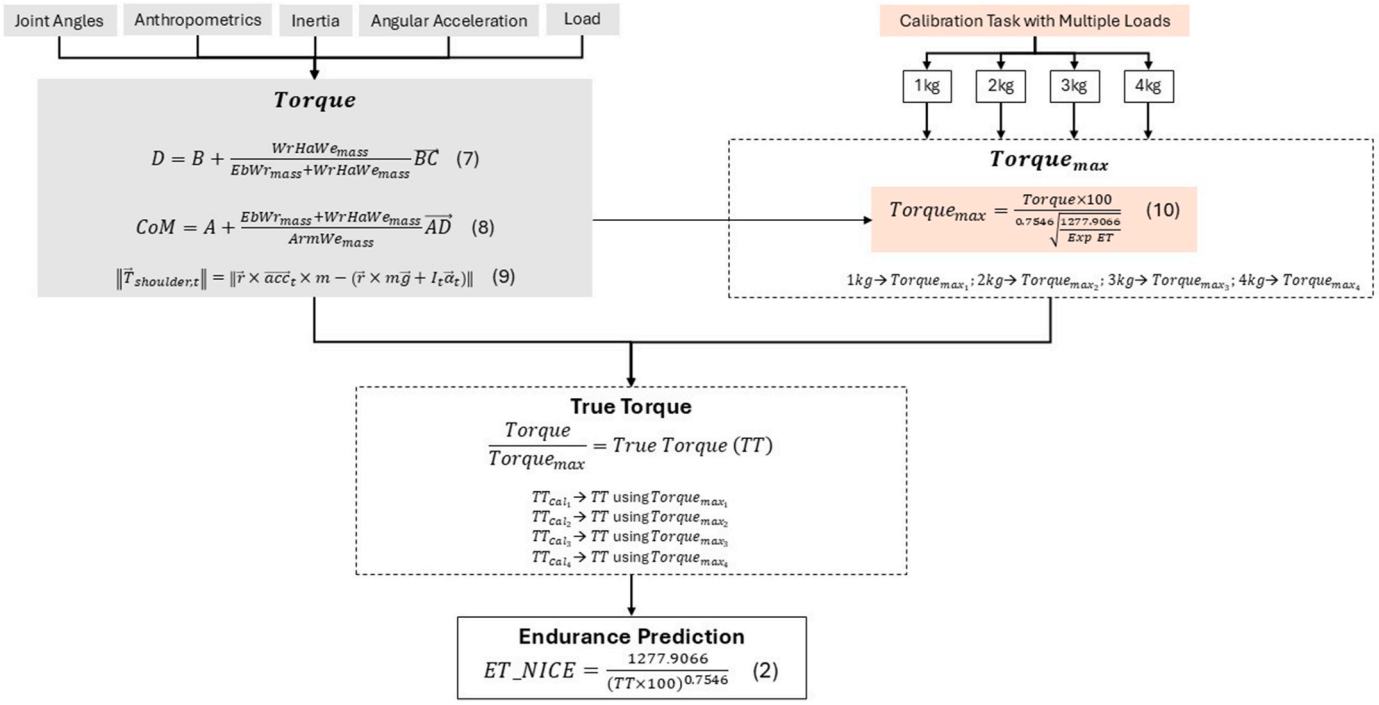


Fig. 8. Recommended use of calibration method to determine an individualised maximum torque value for endurance prediction.

models were compared to reduce ET prediction errors. Static calibration tasks should be completed with multiple loads and the $Torque_{max}$ corresponding to the load in a manual handling task should be used to predict ET, Fig. 8. This work established an easily reproducible approach to achieve reduced ET errors that take an individual's fatigability at each SI into account. However, these results may not provide optimal $Torque_{max}$ for tasks other than lifting; different calibration tasks may be more appropriate depending on the specific type of task for which endurance is being estimated. This study offered a significant contribution when modelling endurance with *Torque* for loaded dynamic tasks and provided an alternative approach to measuring $Torque_{max}$ leading to lower errors and a basis to potentially reduce ET prediction errors in more complex tasks.

4.8. Future research

The limitations can be addressed by exploring alternative $Torque_{max}$ measurement methods and considering posture, individual factors, measured distances to joint centres, applicability to tasks with increased complexity, one-handed versus two-handed tasks and cumulative fatigue using the dataset (O'Sullivan, 2024). Wearables and computer vision have been used with ergonomic risk assessments (Battini et al., 2022), (Stefana et al., 2021) and muscle models (Jang et al., 2017), (Yu et al., 2019) and may aid in adapting the present work to real tasks and work environments. Although a system incorporating endurance models, IMUs for motion tracking, and pressure insoles for external load estimation could enable fatigue forecasting (Kheiri et al., 2023), (Lim and D'Souza, 2020), further research is needed. The results contribute to proactive evaluation of work tasks and may help refine endurance models and ergonomic assessments. By improving fatigue predictions, this research supports future advancements in workplace safety and injury prevention, paving the way for more advanced risk assessments and fatigue monitoring solutions.

5. Conclusion

Six models and four methods of measuring $Torque_{max}$ were used to predict ET of 29 subjects under static and dynamic conditions at low and medium SIs. Predictions varied greatly depending on the $Torque_{max}$ employed. A calibration task which determined the optimal $Torque_{max}$ and the *NICE* model produced the lowest RMSEs. For all tasks, the mean RMSE was reduced from 41.08 s for the best model without the calibration method to 19.11 s using the calibration method for all subjects, from 26.13 s to 12.16 s for males and 51.28 s to 24.45 s for females. Static tasks at a particular load can be used to calibrate an individual for personalized endurance prediction of dynamic tasks and presents opportunities for improved ergonomic risk assessments while laying the foundation for real-time physical fatigue detection with wearables.

CRediT authorship contribution statement

Patricia O'Sullivan: Writing – original draft, Visualization, Methodology, Investigation, Data curation, Conceptualization. **Matteo Menolotto:** Writing – review & editing, Supervision, Methodology, Conceptualization. **Brendan O'Flynn:** Writing – review & editing, Resources, Funding acquisition. **Dimitrios-Sokratis Komaris:** Writing – review & editing, Supervision, Methodology, Conceptualization.

Declaration of competing interest

The authors declare that they have no known competing financial interests or personal relationships that could have appeared to influence the work reported in this paper.

Acknowledgements

This publication has emanated from research conducted with the financial support of Taighde Éireann – Research Ireland under grant number 12/RC/2289-P2 (The Insight Research Centre for Data Analytics), aspects of this research have been supported by 16/RC/3918 (CONFIRM). All work is co-funded under the European Regional Development Fund. For the purpose of Open Access, the author has applied a CC BY public copyright licence to this work.

Appendix A. Supplementary data

Supplementary data to this article can be found online at https://doi.org/10.1016/j.apergo.2025.104480.

References

Åkerstedt, T., Gillberg, M., 1990. Subjective and objective sleepiness in the active individual. Int. J. Neurosci. 52 (1–2), 29–37.

Bałys, P., Buła, P., Dziedzic, D., Uznańska, M., 2020. The future of work in automated warehouse from the perspective of the employees. In: Michałkiewicz, A., Mierzejewska, W. (Eds.), Contemporary Organisation and Management, Challenges and Trends. Wydawnictwo Uniwersytetu Łódzkiego, pp. 267–281. https://doi.org/10.18778/8220-333-2.16.

Battini, D., Berti, N., Finco, S., Guidolin, M., Reggiani, M., Tagliapietra, L., 2022. WEM-Platform: a real-time platform for full-body ergonomic assessment and feedback in manufacturing and logistics systems. Comput. Ind. Eng. 164, 107881. https://doi.org/10.1016/j.cie.2021.107881.

Bispo, L.G.M., Amaral, F.G., 2024. The impact of Industry 4.0 on occupational health and safety: a systematic literature review. J. Saf. Res. 90, 254–271. https://doi.org/10.1016/j.jsr.2024.04.009.

Borg, G.A., 1982. Psychophysical bases of perceived exertion. Med. Sci. Sports Exerc. 14 (5), 377–381.

Bosy-Westphal, A., et al., 2008. Accuracy of bioelectrical impedance consumer devices for measurement of body composition in comparison to whole body magnetic resonance imaging and dual X-ray absorptiometry. Obes. Facts 1 (6). https://doi.org/10.1159/000176061.

Chaffin, D.B., Andersson, G.B., Martin, B.J., 1999. Occupational Biomechanics, third ed. John wiley & sons.

Crawford, J.O., et al., 2020. Musculoskeletal health in the workplace. Best Pract. Res. Clin. Rheumatol. 34 (5), 101558. https://doi.org/10.1016/j.berh.2020.101558.

Dawson, D., Ian Noy, Y., Härmä, M., Åkerstedt, T., Belenky, G., 2011. Modelling fatigue and the use of fatigue models in work settings. Accid. Anal. Prev. 43 (2), 549–564. https://doi.org/10.1016/j.aap.2009.12.030.

Duan, T., et al., 2020. Real-time indicators and influence factors of muscle fatigue in push-type work. Int. J. Ind. Ergon. 80, 103046. https://doi.org/10.1016/j.ergon.2020.103046.

Edwards, R.H.T., 1981. Human muscle function and fatigue. In: Porter, R., Whelan, J. (Eds.), Novartis Foundation Symposia, first ed. Wiley, pp. 1–18. https://doi.org/10.1002/9780470715420.ch1.

El ahrache, K., Imbeau, D., Farbos, B., 2006. Percentile values for determining maximum endurance times for static muscular work. Int. J. Ind. Ergon. 36 (2), 99–108. https://doi.org/10.1016/j.ergon.2005.08.003.

European Agency for Safety and Health at Work, 2022. Third European Survey of Enterprises on New and Emerging Risks (ESENER 2019): How European Workplaces Manage Safety and Health : Overview Report. Publications Office [Online]. Available: https://data.europa.eu/doi/10.2802/881291. (Accessed 9 August 2024).

European Foundation for the Improvement of Living and Working Conditions, 2017. *6th European Working Conditions Survey: 2017 Update.* LU. Publications Office [Online]. Available: https://data.europa.eu/doi/10.2806/422172. (Accessed 1 October 2024).

Freivalds, A., 2011. Biomechanics of the Upper Limbs: Mechanics, Modeling and Musculoskeletal Injuries. CRC press.

Frey Law, L.A., Avin, K.G., 2010. Endurance time is joint-specific: a modelling and meta-analysis investigation. Ergonomics 53 (1), 109–129. https://doi.org/10.1080/00140130903389068.

Gallagher, S., Schall, M.C., Sesek, R.F., Huangfu, R., 2018. An upper extremity risk assessment tool based on material fatigue failure theory: the distal upper extremity tool (DUET). Hum. Factors J. Hum. Factors Ergon. Soc. 60 (8), 1146–1162. https://doi.org/10.1177/0018720818789319.

Garg, A., Hegmann, K.T., Schwoerer, B.J., Kapellusch, J.M., 2002. The effect of maximum voluntary contraction on endurance times for the shoulder girdle. Int. J. Ind. Ergon. 30 (2), 103–113. https://doi.org/10.1016/S0169-8141(02)00078-1.

Garrett, J.W., 1971. The adult human hand: some anthropometric and biomechanical considerations. Hum. Factors 13 (2), 117–131.

Hagberg, M., 1981. Muscular endurance and surface electromyogram in isometric and dynamic exercise. J. Appl. Physiol. 51 (1), 1–7. https://doi.org/10.1152/jappl.1981.51.1.1.

Hart, S.G., Staveland, L.E., 1988. Development of NASA-TLX (Task Load Index): Results of Empirical and Theoretical Research. Adv. Psychol. 52, 139–183. https://doi.org/10.1016/S0166-4115(08)62386-9.

Hincapié-Ramos, J.D., Guo, X., Moghadasian, P., Irani, P., 2014. Consumed endurance: a metric to quantify arm fatigue of mid-air interactions. In: Proceedings of the SIGCHI Conference on Human Factors in Computing Systems. Association for Computing Machinery, New York, NY, USA, pp. 1063–1072. https://doi.org/10.1145/2556288.2557130 in CHI '14.

Hunter, S.K., 2014. Sex differences in human fatigability: mechanisms and insight to physiological responses. Acta Physiol. 210 (4), 768–789.

Hunter, S.K., 2016. The relevance of sex differences in performance fatigability. Med. Sci. Sports Exerc. 48 (11), 2247.

James, S.L., et al., 2018. Global, regional, and national incidence, prevalence, and years lived with disability for 354 diseases and injuries for 195 countries and territories, 1990–2017: a systematic analysis for the Global Burden of Disease Study 2017. Lancet 392 (10159), 1789–1858. https://doi.org/10.1016/S0140-6736(18)32279-7.

Jang, S., Stuerzlinger, W., Ambike, S., Ramani, K., 2017. Modeling cumulative arm fatigue in mid-air interaction based on perceived exertion and kinetics of arm motion. In: Proceedings of the 2017 CHI Conference on Human Factors in Computing Systems. ACM, Denver Colorado USA, pp. 3328–3339. https://doi.org/10.1145/3025453.3025523.

Jebelli, H., Seo, J., Hwang, S., Lee, S., 2020. Physiology-based dynamic muscle fatigue model for upper limbs during construction tasks. Int. J. Ind. Ergon. 78, 102984. https://doi.org/10.1016/j.ergon.2020.102984.

Keyserling, W.M., Brouwer, M., Silverstein, B.A., 1992. A checklist for evaluating ergonomic risk factors resulting from awkward postures of the legs, trunk and neck. Int. J. Ind. Ergon. 9 (4), 283–301. https://doi.org/10.1016/0169-8141(92)90062-5.

Kheiri, S.K., Vahedi, Z., Sun, H., Megahed, F.M., Cavuoto, L.A., 2023. Human reliability modeling in occupational environments toward a safe and productive operator 4.0. Int. J. Ind. Ergon. 97, 103479. https://doi.org/10.1016/j.ergon.2023.103479.

Latko, W.A., Armstrong, T.J., Franzblau, A., Ulin, S.S., Werner, R.A., Albers, J.W., 1999. Cross-sectional study of the relationship between repetitive work and the prevalence of upper limb musculoskeletal disorders. Am. J. Ind. Med. 36 (2), 248–259. https://doi.org/10.1002/(SICI)1097-0274(199908)36:2<248::AID-AJIM4>3.0.CO;2-Q.

Li, K.W., Yi, C., Liu, M., 2021. Maximum endurance time modeling for push and pull tasks considering gender and handle height. Hum. Factors Ergon. Manuf. 31 (1). https://doi.org/10.1002/hfm.20865.

Li, Y., et al., 2023. Revisiting consumed endurance: a NICE way to quantify shoulder fatigue in virtual reality. In: 29th ACM Symposium on Virtual Reality Software and Technology. ACM, Christchurch New Zealand, pp. 1–10. https://doi.org/10.1145/3611659.3615702.

Lim, S., D'Souza, C., 2020. A narrative review on contemporary and emerging uses of inertial sensing in occupational ergonomics. Int. J. Ind. Ergon. 76, 102937. https://doi.org/10.1016/j.ergon.2020.102937.

Lind, C.M., Abtahi, F., Forsman, M., 2023. Wearable motion capture devices for the prevention of work-related musculoskeletal disorders in ergonomics—an overview of current applications, challenges, and future opportunities. Sensors 23 (9), 4259. https://doi.org/10.3390/s23094259.

Liu, J.Z., Brown, R.W., Yue, G.H., 2002. A dynamical model of muscle activation, fatigue, and recovery. Biophys. J. 82 (5). https://doi.org/10.1016/S0006-3495(02)75580-X.

Liu, B., Ma, L., Zhang, W., Zhang, Z., 2019. Subject-specific hand grip fatigability indicator determined using parameter identification technique. Hum. Factors Ergon. Manuf. Serv. Ind. 29 (1), 86–94. https://doi.org/10.1002/hfm.20760.

Lu, L., Megahed, F.M., Sesek, R.F., Cavuoto, L.A., 2017. A survey of the prevalence of fatigue, its precursors and individual coping mechanisms among U.S. manufacturing workers. Appl. Ergon. 65, 139–151. https://doi.org/10.1016/j.apergo.2017.06.004.

Luopajärvi, T., Kuorinka, I., Virolainen, M., Holmberg, M., 1979. Prevalence of tenosynovitis and other injuries of the upper extremities in repetitive work. Scand. J. Work. Environ. Health 48–55.

Ma, L., Chablat, D., Bennis, F., Zhang, W., 2009. A new simple dynamic muscle fatigue model and its validation. Int. J. Ind. Ergon. 39 (1), 211–220. https://doi.org/10.1016/j.ergon.2008.04.004.

Ma, L., Zhang, W., Hu, B., Chablat, D., Bennis, F., Guillaume, F., 2013. Determination of subject-specific muscle fatigue rates under static fatiguing operations. Ergonomics 56 (12), 1889–1900. https://doi.org/10.1080/00140139.2013.851283.

Madonna, M., Monica, L., Anastasi, S., Di Nardo, M., 2019. Evolution of cognitive demand in the human–machine interaction integrated with industry 4.0 technologies. Presented at the SAFE 2019, pp. 13–19. https://doi.org/10.2495/SAFE190021. Ancona, Italy,.

Martins, N.R.A., Annaheim, S., Spengler, C.M., Rossi, R.M., 2021. Fatigue monitoring through wearables: a state-of-the-art review. Front. Physiol. 12, 790292. https://doi.org/10.3389/fphys.2021.790292.

Mathiassen, S.E., Åhsberg, E., 1999. Prediction of shoulder flexion endurance from personal factors. Int. J. Ind. Ergon. 24 (3), 315–329. https://doi.org/10.1016/S0169-8141(98)00039-0.

McAtamney, L., Corlett, N., 2004. Rapid upper limb assessment (RULA). In: Handbook of Human Factors and Ergonomics Methods. CRC Press, pp. 86–96.

McAtamney, L., Hignett, S., 2004. Rapid entire body assessment. In: Handbook of Human Factors and Ergonomics Methods. CRC press, pp. 97–108.

Neumann, E.E., et al., 2018. Reference data on thickness and mechanics of tissue layers and anthropometry of musculoskeletal extremities. Sci. Data 5 (1), 1–10.

Nussbaum, M.A., Zhang, X., 2000. Heuristics for locating upper extremity joint centres from a reduced set of surface markers. Hum. Mov. Sci. 19 (5), 797–816. https://doi.org/10.1016/S0167-9457(00)00020-8.

O'Sullivan, P., 2024. SWIFTIES (Subject and Wearables Data for Investigation of Fatiguing Tasks in Exension/flexion of Shoulder/elbow), vol. 16. Zenodo. https://doi.org/10.5281/ZENODO.11202227.

O'Sullivan, P., Menolotto, M., O'Flynn, B., Komaris, D.S., 2022. Estimation of maximum shoulder and elbow joint torques based on demographics and anthropometrics. In: 2022 44th Annual International Conference of the IEEE Engineering in Medicine & Biology Society (EMBC). IEEE, Glasgow, Scotland, United Kingdom, pp. 4346–4349. https://doi.org/10.1109/EMBC48229.2022.9870906.

O'Sullivan, P., Menolotto, M., O'Flynn, B., Komaris, D.-S., 2023. Validation of endurance model for manual tasks. In: 2023 45th Annual International Conference of the IEEE Engineering in Medicine & Biology Society (EMBC). IEEE, Sydney, Australia, pp. 1–5. https://doi.org/10.1109/EMBC40787.2023.10341139.

Radwin, R.G., Marras, W.S., Lavender, S.A., 2001. Biomechanical aspects of work-related musculoskeletal disorders. Theor. Issues Ergon. Sci. 2 (2), 153–217. https://doi.org/10.1080/14639220110102044.

Rohmert, W., 1960. Ermittlung von Erholungspausen für statische Arbeit des Menschen. Int. Z. Für Angew. Physiol. Einschließlich Arbeitsphysiologie 18, 123–164.

Rohmert, W., 1973. Problems in determining rest allowances. Appl. Ergon. 4 (2), 91–95. https://doi.org/10.1016/0003-6870(73)90082-3.
Silverstein, B.A., Fine, L.J., Armstrong, T.J., 1987. Occupational factors and carpal tunnel syndrome. Am. J. Ind. Med. 11 (3), 343–358. https://doi.org/10.1002/ajim.4700110310.
Singh, S.N., Rajesh, K.R., Sunil, S., 2022. Ergonomics control – assembly station. Mater. Today Proc. 54, 513–518. https://doi.org/10.1016/j.matpr.2021.11.505.
Snook, S.H., Ciriello, V.M., 1991. The design of manual handling tasks: revised tables of maximum acceptable weights and forces. Ergonomics 34 (9), 1197–1213. https://doi.org/10.1080/00140139108964855.
Stefana, E., Marciano, F., Rossi, D., Cocca, P., Tomasoni, G., 2021. Wearable devices for ergonomics: a systematic literature review. Sensors 21 (3), 777. https://doi.org/10.3390/s21030777.
Steven Moore, J., Garg, A., 1995. The strain index: a proposed method to analyze jobs for risk of distal upper extremity disorders. Am. Ind. Hyg. Assoc. J. 56 (5), 443–458. https://doi.org/10.1080/15428119591016863.
Tan, H.Z., Srinivasan, M.A., Eberman, B., Cheng, B., 1994. Human factors for the design of force-reflecting haptic interfaces. Dyn. Syst. Control 55 (1), 353–359.
Wan, J., Qin, Z., Wang, P., Sun, Y., Liu, X., 2017. Muscle fatigue: general understanding and treatment. Exp. Mol. Med. 49 (10). https://doi.org/10.1038/emm.2017.194.
Waters, T.R., Putz-Anderson, V., Garg, A., Fine, L.J., 1993. Revised NIOSH equation for the design and evaluation of manual lifting tasks. Ergonomics 36 (7), 749–776.
Williamson, A., Lombardi, D.A., Folkard, S., Stutts, J., Courtney, T.K., Connor, J.L., 2011. The link between fatigue and safety. Accid. Anal. Prev. 43 (2), 498–515. https://doi.org/10.1016/j.aap.2009.11.011.
Winter, D.A., 2009. Biomechanics and Motor Control of Human Movement. John Wiley & Sons.
Yi, C., Tang, F., Peng, L., Li, K.W., Ma, L., Hu, H., 2018. Modeling of maximum endurance time for static pulling tasks. Work 60 (3), 455–463.
Yu, Y., Li, H., Yang, X., Kong, L., Luo, X., Wong, A.Y.L., 2019. An automatic and non-invasive physical fatigue assessment method for construction workers. Autom. Constr. 103, 1–12. https://doi.org/10.1016/j.autcon.2019.02.020.
Yung, M., Kolus, A., Wells, R., Neumann, W.P., 2020. Examining the fatigue-quality relationship in manufacturing. Appl. Ergon. 82, 102919. https://doi.org/10.1016/j.apergo.2019.102919.
'Conventional Upper Skeleton Marker Set', Optitrack Conventional Upper (27). Accessed: Dec. 05, 2024. [Online]. Available: https://docs.optitrack.com/markersets/upper/conventional-upper-27.